Geol. Mag. **150** (*3*), *2013, pp. 385–395.* © *Natural Environmental Research Council. Published by Cambridge University Press 2012*
doi:10.1017/S0016756812000325

Silicified serpentinite – a residuum of a Tertiary palaeo-weathering surface in the United Arab Emirates

ALICJA M. LACINSKA* & MICHAEL T. STYLES

British Geological Survey, Kingsley Dunham Centre, Keyworth, Nottinghamshire NG12 5GG, UK

(*Received* 30 August 2011; *accepted* 27 April 2012; *first published online* 29 October 2012)

Abstract – Mineralogical studies of a silicified serpentinite from the United Arab Emirates throw light on the formative processes. The silicified serpentinite is a residuum of a palaeo-weathering surface that probably developed in a temperate climate with alternating wet and dry periods during middle Eocene to late Miocene times. The rock textures indicate that silicification occurred in a fluid-saturated zone. Silica precipitation is favoured at near-neutral pH. In this study we infer that these pH conditions of the mineralizing fluids could arise in a near-surface mixing zone where acidic meteoric and hyperalkaline groundwater fluids are mingled. This mingling is believed to have resulted from alternating processes of evaporation and precipitation that prevailed during dry and wet seasons, respectively. The silicified serpentinite is composed of > 95 % quartz and exhibits a ghost texture of the protolith serpentinite. Preservation of the textures indicates an iso-volumetric grain-by-grain replacement by dissolution of Mg-silicate and simultaneous precipitation of either opal or microquartz as siliceous seeds. These were subsequently overgrown by silica that was probably remobilized from deeply weathered regolith elsewhere.

Keywords: serpentinite, silicification, microquartz, incongruent dissolution, silcrete, Semail Ophiolite.

1. Introduction

The term silicified serpentinite (SiSp) refers here to a dense, ferruginous and siliceous rock that displays clear evidence for pseudomorphic replacement of the protolith serpentinite by quartz. Many authors have reported the existence of SiSp, silicified zones or silcrete formed by subaerial erosion of serpentinite (Rice & Cleveland, 1955; Folk & McBride, 1978; Leblanc & Billaud, 1982; Som & Joshi, 2002 and references therein). A wide range of names have been used to describe these rocks. Molly (1959) referred to an earlier work by Duparc (1927) and described birbirite, which was later referred to as dunite with Mg leached out (Otteman & Augustithis, 1967). Birbirite was further adopted by Glennie *et al*. (1974) to describe a silicified crust that overlies partially serpentinized peridotite at the western edge of the northern Oman Mountains. Glennie *et al*. (1974) also introduced the term Amqat for silicified serpentinite that stands proud of the normal serpentinite topography in the Oman Mountains. The Amqat unit is situated exclusively within the basal serpentinite, locally adjacent to a basal thrust (Stanger, 1985), as opposed to birbirite, which overlies the serpentinite. Nasir *et al*. (2007) included both birbirite and Amqat in listwaenite – a term that the authors referred to as an intensively carbonate- and silica-altered mafic and ultramafic rock. These rocks are reported to be of hydrothermal origin.

In this paper, we suggest that the silicified serpentinite in the United Arab Emirates (UAE) that lies in a different lithological setting (see Section 3) to Amqat resulted from weathering of serpentinite and ultramafic rocks in a temperate climate. Based on the microtextural and compositional characteristics of the rocks analysed, and in conjunction with our knowledge of the field setting, we add significantly to the discussion of the formative processes.

This publication aims to (a) identify the possible origin of silicification, and (b) propose the most likely time for the formation of silicified serpentinite in the UAE in relation to a palaeoclimate reconstruction by Zachos, Dickens & Zeebe (2008).

2. Theoretical background

Most previous studies of the silicification of serpentinite imply that during weathering, the silica in ferromagnesian minerals is slightly less susceptible to leaching than magnesia (Trescases, 1973; Glennie *et al*. 1974). The mobility of other elements during weathering of ultramafic rocks follows the order: Ca > Mg > Si > Ni > Co ≈ Zn ≈ V > Fe = Cr ≈ Mn (Venturelli, Contini & Bonazzi, 1997). Ca and Mg are readily mobilized and complexed with bicarbonate (Bassett, 1954).

Barnes *et al*. (1973) investigated the geochemical processes of silicification in relation to silica-carbonate-altered serpentinite. According to Barnes *et al*. (1973), the gaseous CO_2 present in the environment controls the meteoric/groundwater pH (Eq. (1)) and causes serpentine/olivine to yield Mg^{2+}, Fe^{2+} and silica into solution.

$$\begin{aligned} CO_2 + H_2O &\rightarrow H^+ + HCO_3^- \\ HCO_3^- &\rightarrow H^+ + CO_3^{2-} \end{aligned} \quad (1)$$

*Author for correspondence: alci@bgs.ac.uk

(*a*) *Serpentine*

$$6H^+ + Mg_3Si_2O_5(OH)_4 \rightarrow 3Mg^{2+} + 2H_4SiO_4 + H_2O$$

(*b*) *Olivine*

$$4H^+ + Mg_2SiO_4 \rightarrow 2Mg^{2+} + H_4SiO_4 \quad (2)$$

The equations show that there are two competing processes to which the system is exposed: one which yields H^+ ions to the environment due to CO_2 dissolution in water (Eq. (1)) and the other related to the consumption of H^+ ions due to the reaction with serpentinite (Eq. (2)). These conditions providing the high CO_2 activity – and therefore low pH – enable the serpentinite to yield Mg until all the Mg is exhausted and to form a silica residuum (Barnes *et al*. 1973). Fe and Cr are the less mobile elements and remain as a secondary Fe oxyhydroxide and primary chromite, respectively. The silica-rich residuum can either bond with, if present in sufficient quantities, Fe, Ca, Al and remaining Mg to form clay minerals and/or more likely become oversaturated and precipitate *in situ* as amorphous silica or crystalline quartz.

The dissolution of ferromagnesian minerals has been the subject of many experimental studies, including the reactions of serpentine, forsterite and enstatite (Luce, Bartlett & Parks, 1972) and fayalite and hyperstene (Siever & Woodford, 1979) with solutions of various pHs (mainly < 7) at 25 °C. The experiments of Luce, Bartlett & Parks (1972) showed that the initial dissolution is incongruent and related to rapid exchange of surface Mg^{2+} with H^+ ions. This rapid exchange is then followed by nearly congruent dissolution that allows the extraction of internal Mg and Si. Siever & Woodford (1979) confirmed the suggestion of Barnes *et al*. (1973) that these minerals dissolve more rapidly at lower pH and that the dissolution is sequential. The following reaction steps were distinguished: (1) exchange reaction between Mg^{2+}, Fe^{2+} with H^+; (2) incongruent dissolution of the silicate structure; (3) oxidation of Fe^{2+} to Fe^{3+}; (4) precipitation of $Fe(OH)_3$; and (5) scavenging of cations and silica by newly precipitated $Fe(OH)_3$.

3. Geological setting

The UAE–Oman ophiolite is the world's largest and one of the best exposed ophiolite complexes, forming the Hajar Mountains along the NE margin of the Arabian plate. Detailed mapping of the Hajar Mountains in the UAE by the British Geological Survey has shown that SiSp outcrops form an almost continuous horizon along the western margin of the UAE–Oman ophiolite (Styles *et al*. 2006) (Fig. 1). The outcrops occur in a transition zone between mountainous terranes and flat plains of the encroaching desert sand. The SiSp is everywhere underlain by serpentinite and variably serpentinized harzburgite. There is normally a clear transition from completely serpentinized rock, up to about 10 m thickness, passing down into less serpentinized harzburgite. All the units are cross-cut by fractures filled with various amounts

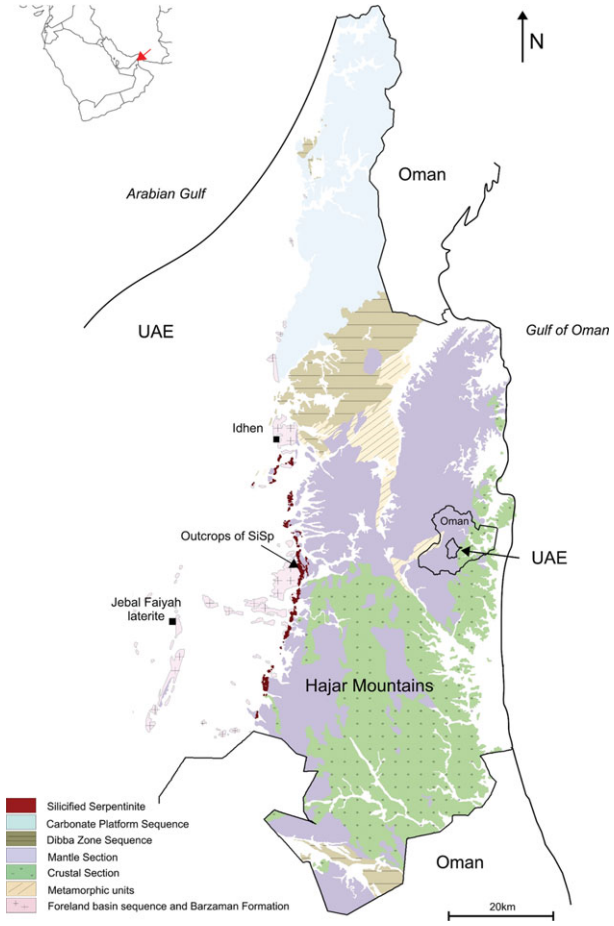

Figure 1. (Colour online) Simplified geological map showing the distribution of silicified serpentinite (dark red) along the western part of Hajar Mountains (after Styles *et al*. 2006). The map also shows the locality of Late Cretaceous/early Tertiary laterites at Jebal Faiyah.

of magnesite, dolomite, calcite, gypsum, silica and serpentine minerals. The fractures are most frequent near to the SiSp–serpentinite contact and decrease in frequency with depth. The thickness of the SiSp unit varies from locality to locality but usually ranges from 1 to 5 m.

In outcrop, the SiSp is dark orange to rusty brown, dense and very hard; resisting weathering to form positive topographic features (Fig. 2). The SiSp is cross-cut by usually <50 mm wide fractures that are partially to completely sealed by either silica and/or carbonate. Variable amounts of magnesite, dolomite, calcite and colour-banded, waxy to vitreous chalcedony and quartz were identified. The fracture system is multigenerational and involves composite events of alternating carbonate and chalcedony mineralization that clearly post-date the silicification. The SiSp fracture surfaces are locally covered by <10 mm in diameter, rosette-like clusters of small (<2 mm) prismatic crystals of quartz that grew perpendicular to the nucleation surface.

Samples from the western edge of the Hajar Mountains (Fig. 1) were examined in the British

https://doi.org/10.1017/S0016756812000325 Published online by Cambridge University Press

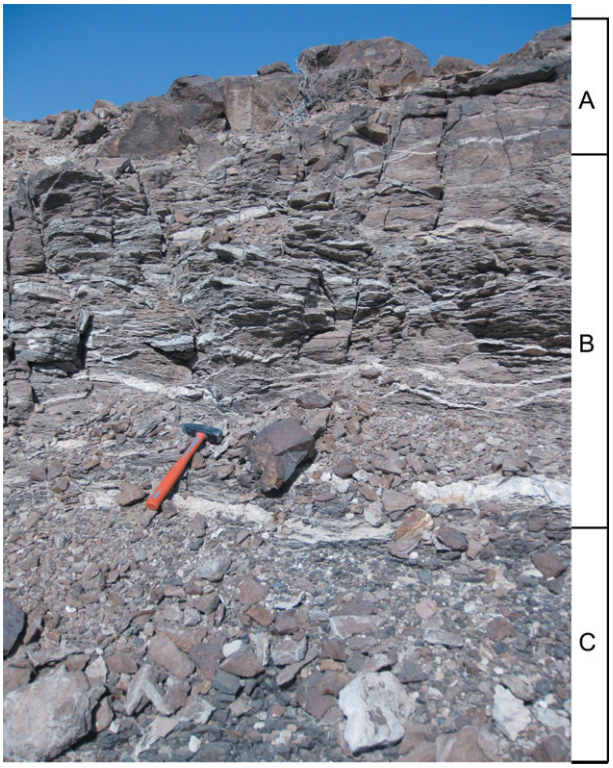

Figure 2. (Colour online) Image showing field relation between the silicified serpentinite (A) and underlying veined and brecciated serpentinite (B) and harzburgite (C). The harzburgite (black colour) is largely covered by the SiSp and Sp scree. Table 1 contains related XRD data (profile 2).

Geological Survey laboratories. The samples are from areas previously described as birbirite by Glennie *et al*. (1974). The rocks directly overly the ophiolite and are locally overlain by dolomite-cemented, ophiolite-derived conglomerates of the Barzaman Formation (Styles *et al*. 2006). They are not in the basal thrust zone of the ophiolite as are the listwaenites described by Nasir *et al*. (2007) and are in a totally different setting to Amqat that has exclusively formed from the basal serpentinite (Glennie *et al*. 1974). A simplified cross-section through the Hajar Mountains and adjacent lithologies (Fig. 3) shows the setting of SiSp in comparison with the listwaenite located in the basal thrust zone of the ophiolite.

The term silicified serpentinite (SiSp) will be used for the rock and microquartz for the dominant mineral. The term microquartz is entirely descriptive and has no generic implications (Flörke *et al*. 1991). It describes a microcrystalline variety of quartz with a granular texture that displays a random mutual orientation of strained grains ($<20\ \mu$m) and usually displays undulatory extinction when observed under a petrographic microscope.

4. Analytical techniques

Description of textural and mineralogical characteristics was completed using a petrographical microscope and scanning electron microscope (SEM). Mineralogical data were obtained from X-ray diffraction analysis (XRD). Major and trace element concentrations were determined by a combination of X-ray fluorescence analysis (XRF) and Na_2O_2 fusion inductively coupled plasma-mass spectrometry (ICP-MS).

The SEM analysis was performed using a LEO 435VP variable pressure digital SEM. The instrument was equipped with a KE Developments four-quadrant (4 diode-type) solid-state detector for backscattered electron imaging (BSEM). Phase/mineral identification

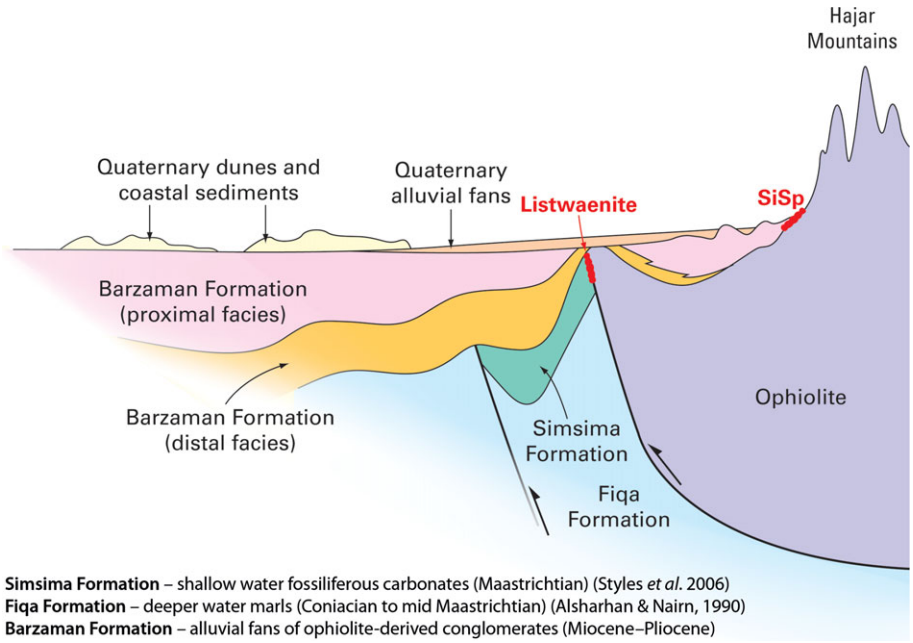

Figure 3. (Colour online) Simplified cross-section through the Hajar Mountains and adjacent lithologies showing the position of the SiSp in relation to listwaenite that occurs in the basal thrust zone.

https://doi.org/10.1017/S0016756812000325 Published online by Cambridge University Press

was aided by qualitative observation of energy-dispersive X-ray spectra recorded simultaneously during SEM observation, using an Oxford Instruments INCA energy-dispersive X-ray microanalysis (EDXA) system.

A Zeiss Axioplan 2ie optical microscope, with digital photomicrographs captured with a Zeiss Axiocam MRc5 digital camera, was used for petrographical analysis.

The XRD analysis was carried out using a PANalytical X'Pert Pro series diffractometer equipped with a cobalt-target tube, X'Celerator detector and operated at 45 kV and 40 mA. The spray-dried samples were scanned from 4.5–85°2θ at 2.76°2θ/minute. Diffraction data were initially analysed using PANalytical X'Pert Highscore Plus version 2.2a software coupled to the latest version of the International Centre for Diffraction Data (ICDD) database. Following identification of the mineral species present in the samples, mineral quantification was achieved using the Rietveld refinement technique (e.g. Snyder & Bish, 1989) using PANalytical Highscore Plus software.

The ICP-MS analysis was carried out using an Agilent 7500cx instrument. The samples were fused in glassy carbon crucibles with sodium peroxide in a ratio of sample:flux of 1:4. The fused material was solubilized in dilute HCl acid and a trace of HF to ensure dissolution of high-field-strength elements (HFSEs), such as tantalum and silica, with the solution being stored in LDPE bottles until required. On the day of analysis by ICP-MS, the samples were diluted to a total factor of 5000. Calibration was achieved using a series of synthetic chemical standards in Na_2O_2 matrix-matched solutions. Chemical quality control standards were similarly prepared but sourced from a different manufacturer. Blank and reference material (BCR-2 and AGV-2) fusions were also analysed to check on accuracy. For XRF analysis, performed using PANalytical Axios Advance, the samples were dried overnight at 105 °C before analysis. Loss on ignition was determined after 1 hour at 1050 °C. Fe_2O_3t represents total iron expressed as Fe_2O_3. F, Cl and SO_3 represent fluorine, chlorine and sulphur retained in the fused bead after fusion at 1200 °C. The samples were fused in a mixed lithium tetraborate/lithium metaborate flux in a ratio of sample:flux of 1:10 and cast into 40 mm glass beads for analysis by wavelength dispersive XRF spectrometry.

5. Petrography and mineralogy

In thin-section, the SiSp displays a characteristic meshwork texture of rounded, <1 mm domains of microquartz that are irregularly intermixed with stringers and patches of haematite and goethite (Figs 4, 5). The domains are composed of tightly packed, anhedral, <5 μm crystals of quartz that display undulatory extinction. The domains are commonly cross-cut by randomly oriented micro-fractures that are filled with fibrous chalcedony. This pattern mimics the mesh texture of the original serpentinites. In addition there are numerous randomly distributed crystals of euhedral chromite (usually <500 μm), some of which are moderately altered from reddish brown, typical of fresh peridotite/serpentinite, to black. In some places chromite crystals have a characteristic, irregularly distributed alteration rim composed of quartz that probably represents pseudomorphic transformation of a former alteration product, probably chlorite (a feature seen in many of the ophiolite peridotites).

The presence of chromite crystals together with the ghost mesh texture indicates that the original rock was a serpentinized peridotite. The rounded domains are probably after the relics of the original olivine crystals in the partially serpentinized peridotite.

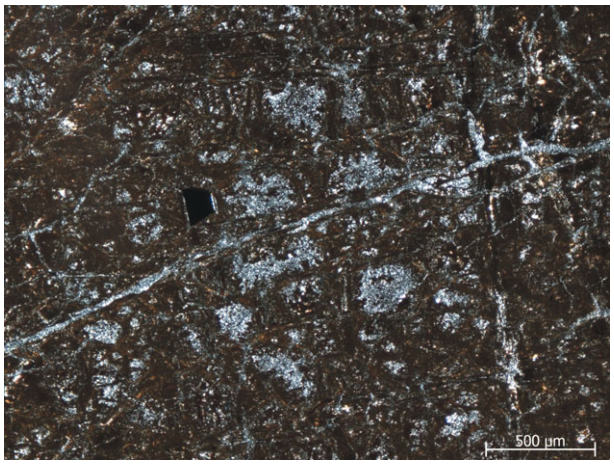

Figure 4. (Colour online) Thin-section photomicrograph of the silicified serpentinite (crossed polars). The rounded to sub-rounded domains of microquartz are probably pseudomorphs after olivine or serpentinized olivine. The rock is brown-stained owing to presence of goethite and haematite. Opaque, angular crystal is chromite.

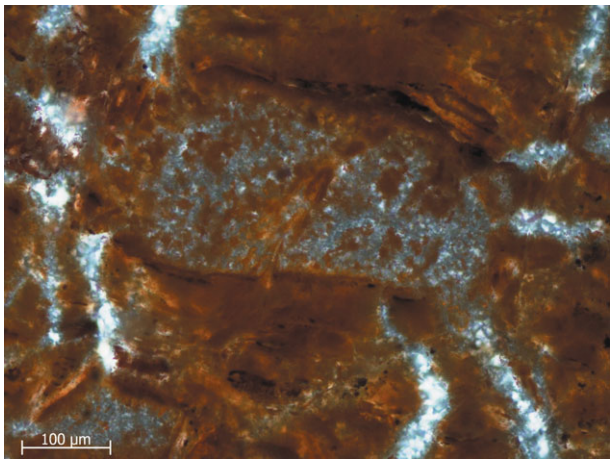

Figure 5. (Colour online) High magnification thin-section photomicrograph (crossed polars) showing a domain of microquartz that is inter-grown with goethite and haematite. This is a former crystal of olivine or serpentinized olivine that, during Mg-silicate–silica transformation, evolved into a siliceous micro-seed.

https://doi.org/10.1017/S0016756812000325 Published online by Cambridge University Press

Table 1. Summary of quantitative whole-rock X-ray diffraction analysis on selected samples

		Mineralogy (%)																
		amphibole	ankerite	calcite	chlorite	clinopyroxene (diopside)	dolomite	enstatite	forsterite	goethite	haematite	serpentine	magnesio-chromite	magnesio-ferrite	'mica'	quartz	quartz normalized*	serpentinite normalized*
Profile 1	SiSp			0.5			14.3				<0.5	0.6	<0.5		0.7	83.8	97.6	
	Sp						16.5			2.3		80.7				0.5		96.7
	Hzb/Lhz	6.2			2.8	5.8	0.5	22.0	53.9			8.4				<0.5		
Profile 2	SiSp (A)	4.0	0.5				24.5		0.8	0.5			0.5			69.4	97.4	
	Sp (B)			22.1	8.7						1.4	67.3	<0.5			<0.5		89.2
	Sp Prd (C)						<0.5	<0.5	12.7		<0.5	85.9				0.5		85.9
	SiSp			0.5			0.5			1.0	<0.5				1.6	96.4	96.4	
	SiSp		4.6	2.0			34.6				0.8	1.3		<0.5	0.9	55.4	95.6	

'mica' – undifferentiated mica species including muscovite, biotite, illite and illite/smectite, etc.
*the amount of mineral after normalization for carbonate. The carbonate present in the samples is in the form of late veins
Sp – serpentinite; Sp Prd – serpentinized peridotite; SiSp – silicified serpentinite; Hzb – harzburgites.
Profile 1 – samples from outcrops south of Idhen.
Profile 2 – samples from outcrops near Oman border (A, B, C – see Fig. 2). The sample of Sp peridotite analysed appeared to be largely serpentinized; the data are shown here for the consistency of the publication only.

The XRD analysis shows that the SiSp consists of >95 % quartz and <2 % haematite and goethite (Table 1). Additionally, small amounts of magnesiochromite, serpentine and undifferentiated clay minerals including illite and illite–smectite were identified. For comparison, the ophiolite directly beneath the SiSp was analysed, and these results are also listed in Table 1. The analysis confirms a major compositional change from peridotite and serpentinized peridotite (ophiolite) to SiSp. In some places the SiSp and serpentinite contain significant amounts (up to 35 %) of carbonate minerals that occur in cross-cutting veins (see Section 3). The veins post-date the silicification and are therefore treated here as additional phases in relation to the original composition of the rock. The tabulated data thus also present values where the 'additional phases' have been removed and the original components normalized. Major and trace element concentrations were obtained by XRF and ICP-MS for three SiSp samples (Table 2). The chemical data agree well with mineralogical and petrographical observations and show a predominance of SiO_2 (up to 81.68 %) and Fe_2O_3t (up to 5.76 %), corresponding to quartz and haematite, respectively. The discrepancy in the amount of mineral phase determined by XRD and the component% obtained from XRF + ICP-MS arises from sample heterogeneity. Relatively high values of MgO (up to 4.75 %) and CaO (up to 7.13 %) are related to the presence of late dolomite and calcite veins.

5.a. Processes of magnesium removal

Previous investigations in the study area showed that the degree of ophiolite serpentinization varies from 25–100 % (Styles *et al*. 2006). Serpentinization is a complex, multistage process that probably starts with the intensive hydration of ultramafic rocks that accompanies obduction of the ophiolite. The process continues with various phases of water ingress, particularly associated with fault zones and post-obduction tectonic events. Finally, there is near-surface hydration by groundwater and meteoric water that continues to the 'present day' (Barnes & O'Neil, 1978) and accompanies subaerial weathering. The field relations of the rocks studied here show clear superposition of a thin, totally serpentinized zone above partially serpentinized harzburgite. This clear lithological superposition suggests aerial to subaerial weathering of harzburgite to serpentinized harzburgite and serpentinite. These rocks were subsequently extensively silicified.

Stanger (1985) suggested that anhydrous phases within the protolith ultramafic rocks (olivine, pyroxene) will react with coexisting low-temperature fluids to form serpentine minerals and yield high pH solutions. The high pH would, in turn, strongly affect the solubility of silica as it increases significantly above pH 9. This implies that the rocks must have been completely serpentinized prior to silicification to enable the precipitation of silica (Stanger, 1985) or a combination of factors occurred that lowered the pH of the mineralizing fluids. The study on nickel laterites in Brazil (Barros de Oliveira, Trescases & Melfi, 1992) showed, however, that olivine had been dissolved with nearly total removal of Mg and partial removal of silica but had not been fully serpentinized. The mouldic cavities of olivine are now filled with amorphous or poorly crystalline iron and nickel phases and silica.

Many researchers (Trescases, 1973; Glennie *et al*. 1974; Barros de Oliveira, Trescases & Melfi, 1992 and references therein) stated that the preferential leaching

https://doi.org/10.1017/S0016756812000325 Published online by Cambridge University Press

Table 2. Major and trace element analyses of SiSp from the UAE

		SiSp I	SiSpII	SiSpIII			SiSpI	SiSpII	SiSpIII
MAJOR					**As**	ppm	0.9	0.8	1.3
SiO_2	%	81.68	80.4	71.25	**Se**	ppm	<4.0	<4.0	<4.0
TiO_2	%	<0.01	<0.01	<0.01	**Rb**	ppm	0.5	<0.4	<0.4
Al_2O_3	%	0.14	0.18	0.04	**Sr**	ppm	402	129	56
Fe_2O_3t	%	3.68	5.31	5.76	**Y**	ppm	0.1	0.3	0.4
Mn_3O_4	%	0.05	0.08	0.07	**Zr**	ppm	<3.0	6.0	<3.0
MgO	%	3.27	3.73	4.75	**Nb**	ppm	<0.1	<0.1	<0.1
CaO	%	3.5	3.25	7.13	**Mo**	ppm	0.4	0.6	0.3
Na_2O	%	<0.05	<0.05	<0.05	**Ag**	ppm	<0.2	<0.2	<0.2
K_2O	%	0.01	0.05	<0.01	**Cd**	ppm	<0.1	<0.1	<0.1
P_2O_5	%	<0.01	<0.01	<0.01	**Sn**	ppm	<1.0	<1.0	<1.0
SO_3	%	0.30	0.20	0.60	**Sb**	ppm	<0.1	<0.1	<0.1
Cr_2O_3	%	0.51	0.26	0.05	**Cs**	ppm	<0.05	<0.05	<0.05
SrO	%	0.03	<0.01	<0.01	**Ba**	ppm	14.0	82.0	35.0
ZrO_2	%	<0.02	<0.02	<0.02	**La**	ppm	<0.6	<0.6	<0.6
BaO	%	<0.02	<0.02	<0.02	**Ce**	ppm	<4.0	<4.0	<4.0
NiO	%	0.07	0.11	0.12	**Pr**	ppm	<0.3	<0.3	<0.3
CuO	%	<0.01	<0.01	0.10	**Nd**	ppm	<1.0	<1.0	<1.0
ZnO	%	<0.01	<0.01	<0.01	**Sm**	ppm	<0.2	<0.2	<0.2
PbO	%	<0.01	<0.01	<0.01	**Eu**	ppm	<0.1	<0.1	<0.1
V_2O5	%	<0.01	<0.01	0.01	**Gd**	ppm	<0.05	<0.05	0.05
HfO_2	%	<0.01	<0.01	<0.01	**Tb**	ppm	<0.05	<0.05	<0.05
F	%	<0.1	<0.1	<0.1	**Dy**	ppm	<0.05	<0.05	0.05
Cl	%	<0.1	<0.1	<0.1	**Ho**	ppm	<0.05	<0.05	<0.05
LOI	%	6.22	6.01	10.13	**Er**	ppm	<0.05	<0.05	<0.05
Total	%	99.46	99.58	100.01	**Tm**	ppm	<0.05	<0.05	<0.05
TRACES					**Yb**	ppm	<0.05	<0.05	<0.05
Li	ppm	7.0	15.0	4.0	**Lu**	ppm	<0.05	<0.05	<0.05
Be	ppm	<0.4	<0.4	<0.4	**Hf**	ppm	<0.1	0.1	<0.1
B	ppm	<30	<30	<30	**Ta**	ppm	<0.1	<0.1	<0.1
P	ppm	<100	121	<100	**W**	ppm	<1.0	<1.0	<1.0
Ti	ppm	<50	<50	<50	**Tl**	ppm	<0.1	<0.1	<0.1
V	ppm	22	38	53	**Pb**	ppm	<0.7	<0.7	<0.7
Cr	ppm	3392	1704	300	**Bi**	ppm	<0.1	<0.1	<0.1
Mn	ppm	380	576	484	**Th**	ppm	1.0	<0.6	<0.6
Co	ppm	49	70	72	**U**	ppm	0.14	1.78	0.47
Ni	ppm	547	799	871	**Au∗**	ppb	<1.0	<1.0	<1.0
Cu	ppm	3.7	7.0	3.4	**Pt∗**	ppb	1.8	3.5	1.0
Zn	ppm	20.0	24.0	8.0	**Pd∗**	ppb	1.2	0.7	0.01
Ga	ppm	<1.0	<1.0	<1.0	**Rh∗**	ppb	1.26	1.11	0.3

The relatively high values of MgO and CaO determined are related to the presence of carbonates (dolomite and probably calcite) that occur in post-dating veins.
∗ The values for Au, Pt, Pd and Rh are derived from an earlier study of M. Styles *et al*. (unpub. British Geological Survey Internal Report, CR/11/014, 2011).

of Mg is the primary process that leads to silicification of serpentinite, the Mg being mobilized and removed from the system. It appears likely, but is not a certainty, that the rocks analysed for the current work were fully serpentinized prior to silicification. This is why the transformation of both hydrous and anhydrous phases will be considered below.

The explanation for the liberation of Mg from either hydrous or anhydrous ferromagnesian silicates lies within the internal structure of the mineral, i.e. structure complexity–organization of polyhedrons, arrangement of atoms within the octahedral and tetrahedral sites, and atomic bonds. Here we give insights into how these factors might have affected the release of Mg; however, this will be a subject of future investigation. Serpentine and olivine (forsterite) will be considered as representative minerals of the hydrous and anhydrous minerals, respectively. Serpentine and forsterite are Mg-rich silicates, some forms containing up to a few wt. % of additional Fe^{2+}, Fe^{3+} and Al^{3+} and traces of Ni^{2+} and Mn^{2+}. The structure of olivine consists of isolated Si–O tetrahedra and octahedrally coordinated Mg and Fe cations. Serpentine minerals are layer silicates that consist of layers (sheets) of polymerized SiO_4^{4-} tetrahedra that are attached to layers of $Mg(OH)_2$ octahedra. In general, in both serpentine and olivine, the Mg–O atoms in the octahedra are bound weakly by ionic bonds in comparison to the stronger, partially covalent Si–O bonds in the tetrahedra.

It has been reported that upon protonation (addition of H^+) of the surface layer of olivine, the weak Mg–O bonds lengthen, making them even weaker and prone to breaking (Pokrovsky & Schott, 2000; Liu, Olsen & Rimstidt, 2006). In addition, the Mg atoms, which are coordinated by 6 oxygen atoms, have Pauling bond strengths of 0.33, while the tetrahedrally coordinated Si atoms have Pauling bond strengths of 1.0 (Rosso & Rimstidt, 2000). This implies that the Mg–O bonds are easier to break than the Si–O bonds. Furthermore, the isolated SiO_4 tetrahedra in the olivine structure, as opposed to polymerized Si–O tetrahedra in the serpentine or pyroxene minerals, make them more

https://doi.org/10.1017/S0016756812000325 Published online by Cambridge University Press

vulnerable to transformation; thus, olivine tends to dissolve more readily. The preferential release of Mg^{2+} and Fe^{2+} occurs during the initial stages of dissolution. In general the prolongation of hydrolysis leads to complete dissolution of olivine or serpentine minerals, and, at the end of the reaction, either weakly dissociated silicic acid or neutral silica is released (Eq. (2a, b)). Whether the dissolution is congruent or not is still debatable and probably dependent on the formation of a solid residuum in a long-term process.

5.b. Mechanisms of microquartz formation in the SiSp

In the current study it appears that the SiSp has formed in the course of incongruent dissolution processes, with complete release of Mg^{2+} and Fe^{2+} into the solution and formation of a solid silica residuum that preserved the original serpentinite mesh texture. XRD analysis revealed that the SiSp is composed of > 95 % quartz. This implies that whatever intermediate process took place in between removal of cations and the formation of microquartz, it resulted in high crystallinity and not an amorphous material. Olivine and serpentine are not iso-structural with quartz; thus, isomorphic substitutions are not possible. Furthermore, a large-scale recrystalization of the whole rock to microquartz would involve textural rearrangement. If recrystalization has happened in the rocks studied, it has largely been on a micron-scale, as many ghost textures are preserved. Annealing of an amorphous form would probably achieve this.

Two possible mechanisms for the formation of microquartz in the SiSp are proposed:

(1) Rapid precipitation of quartz from solution with numerous centres of nucleation. This is supported by the micro-morphological characteristic: a rigid mosaic of microcrystalline $<5\ \mu$m, anhedral but usually equigranular quartz. The centres of nucleation could be the relics of the original mineral phases.

(2) Deposition of amorphous silica from supersaturated solutions or direct formation of amorphous silica during acid leaching of serpentine and subsequent transformation of the less crystalline opal-C/CT to quartz. The mechanism behind this transformation is still unclear, but it appears that it occurs by means of dissolution–precipitation (Stein & Kirkpatrick, 1976; Williams, Parks & Crerar, 1985) with concurrent ordering of the structure and removal of water.

Irrespective of the initial process, the original minerals (serpentine, olivine) have disappeared completely and the newly formed quartz preserves the original serpentinite mesh texture, suggesting that the transformation of Mg-silicate to silica was iso-volumetric. There is no evidence for major reorganization of the original rock fabric.

6. Palaeoclimate implications

The reactions that take place during the dissolution of serpentine, in common with other silicates, have been studied widely and the studies imply that the processes are significantly enhanced in a hot and humid climate. Under tropical conditions, serpentinite weathers extensively to produce a thick layer of residual lateritic regolith (Trescases, 1973; Nickel & Thornber, 1977; Barros de Oliveira, Trescases & Melfi, 1992 and references therein). CO_2 dissolved in rainwater, combined with CO_2 originating from oxidation of organic matter in the soil, produces acidic conditions in which the silicate structure is unstable and undergoes leaching and possibly disintegration. The readily mobilized elements, i.e. Mg, Ca and Si, are removed from the system leaving behind a porous, deeply weathered ferruginous residuum: a lateritic soil (Fig. 6).

The SiSp does not show any textural features suggesting that it has formed in soils. No soil-like textures were observed, i.e. colour mottling, fossilized rootlets, nodules or characteristics of an unsaturated horizon, such as pendant cement fabric. On the contrary, the rock displays roughly homogenous mineral growth fabrics, which suggest that they formed in fully fluid-saturated pores. As mentioned above, the pH of the environment that leads to formation of lateritic soil is considered to be too low for any silica form to be stable, as it tends to be deposited in near-neutral pH environments (Schaetzl & Anderson, 2005). Silica solubility is greatest at pH > 9 and <4. The high activity of H^+ in the lateritic soil arises from the dissolution of atmospheric CO_2, activity of organic matter and to a lesser extent, decomposition of sulphides (Nickel & Thornber, 1977). On the other hand, the groundwater emerging from harzburgite and serpentinite-dominated bedrock is known to be hyperalkaline (Barnes & O'Neil, 1969; Stanger, 1985) and therefore also unsuitable for any form of silica mineral to form. Considering the pH, fluid saturation level and the microtextures within the SiSp, we infer that the silicification might have occurred in the fluid-saturated mixing zone (the phreatic zone). The near-neutral pH of the fluids in this zone can be attributed to counterbalancing reactions that take place during the mingling of meteoric (low pH) and groundwater (high pH) fluids. The high activity of soil H^+ is balanced by ongoing *in situ* dissolution of silicates and serpentinization of the remnants of olivine and pyroxene by groundwater.

In the phreatic zone, the fluids are probably less acidic (lower degree of soil H^+ activity); thus, the rate of dissolution of Mg-silicates could potentially be slower. Some of the silica might have been retained in the system by immediate *in situ* precipitation and formation of siliceous micro-seeds that ghost the crystals of serpentinized olivine (Figs 5, 6). This is achieved by local silica-oversaturation that resulted from the preferential mobilization of Mg from dissolving Mg-silicates. The processes of dissolution of Mg-silicates and the precipitation of silica might have occurred simultaneously. Nickel & Thornber (1977) reported that the silicification developed preferentially over

https://doi.org/10.1017/S0016756812000325 Published online by Cambridge University Press

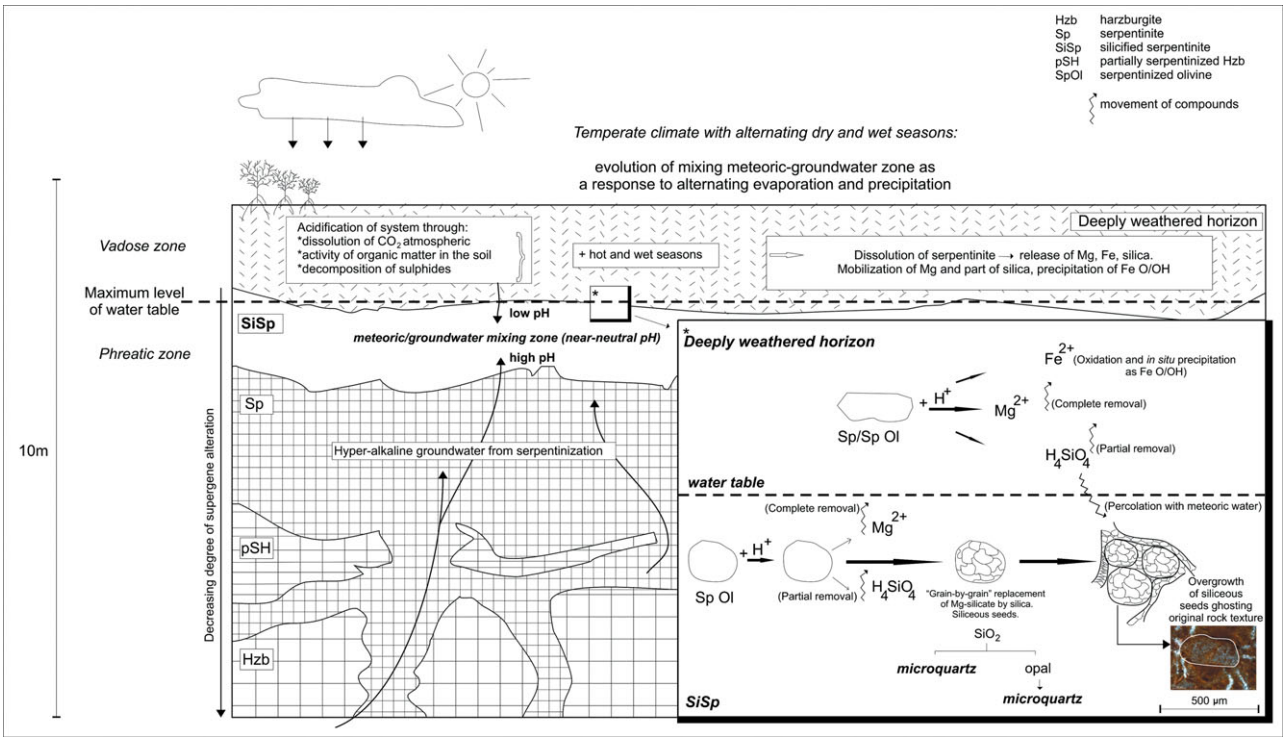

Figure 6. (Colour online) Schematic showing the evolution of conditions that could have prevailed during the formation of the SiSp in the UAE.

serpentinite at several localities in Western Australia and suggest that the silica, therefore, was derived from decomposition of serpentinite. The extensive dissolution of the upper part of the weathering profile provided substantial amounts of silica that subsequently percolated to the base of the profile (Bassett, 1954; Thiry & Simon-Coicon, 1996) and precipitated from solution in the favoured near-neutral pH of the fluid-mixing zone. With time, the mobilized silica added to the overall silicification by overgrowing the siliceous seeds whilst maintaining the original textures (Fig. 6). Depending on the degree of silica saturation, opal (supersaturated solutions) or microquartz (less concentrated solutions) precipitated within the micro-seeds (Iler, 1979, pp. 174, 225). The micro-scale, grain-by-grain replacement mechanism that implies slow rates of dissolution and immediate local precipitation explains the well-preserved mesh texture (Williams, Parks & Crerar, 1985). Silica-rich capping was also reported from the Sierra Nevada (Rice & Cleveland, 1955) and attributed to supergene deposition of silica that was presumably derived from lateritic weathering during the early Tertiary Period. There is no direct evidence for the existence of a deeply weathered profile at the localities studied, i.e. laterite. It would, however, have been a friable component of the weathering profile, which would have been eroded away during initial stages of uplift and erosion in the Hajar Mountains.

Our study shows that the SiSp is an indurated siliceous rock formed in the near-surface environment through remobilization of silica from different weathering horizons. From this it can be inferred that the well-exposed SiSp in the UAE is a silcrete.

During weathering of ultramafic rocks in a tropical climate, the extensive and pervasive dissolution of silicates leads to the formation of thick laterite horizons (such as those observed at Jebel Fayah, UAE), but silcrete may only be a thin layer or possibly absent (Thiry & Millot, 1986). By contrast, in a temperate climate the groundwater level will fluctuate as a response to precipitation and evaporation. This in turn would favour the evolution of a meteoric–groundwater mixing zone that would be suitable for the formation of thick silcrete horizons, such as the UAE SiSp. The palaeogeographical setting of the SiSp could play an important role in its formation and distribution. Thiry & Simon-Coincon (1996, 1999) reported that the silcretes are thicker in the transition zones between gently inclined slopes (glacis) and plains and attribute this phenomenon to contribution of lateral flow along the glacis. This is similar to the likely situation in the UAE in the middle Tertiary Period (see Section 3).

7. Timing of silicification

Our inferences concerning the timing of the silicification are based on the textural and lithostratigraphical relationship. Clasts of SiSp are commonly found within the basal layers of the dolomite-cemented Barzaman Formation conglomerate (Styles *et al*. 2006). This indicates that the SiSp formed prior to the main phase of uplift and erosion that caused the accumulation of ophiolitic detritus (including clasts of SiSp) in the Miocene–Pliocene alluvial fans (Barzaman

https://doi.org/10.1017/S0016756812000325 Published online by Cambridge University Press

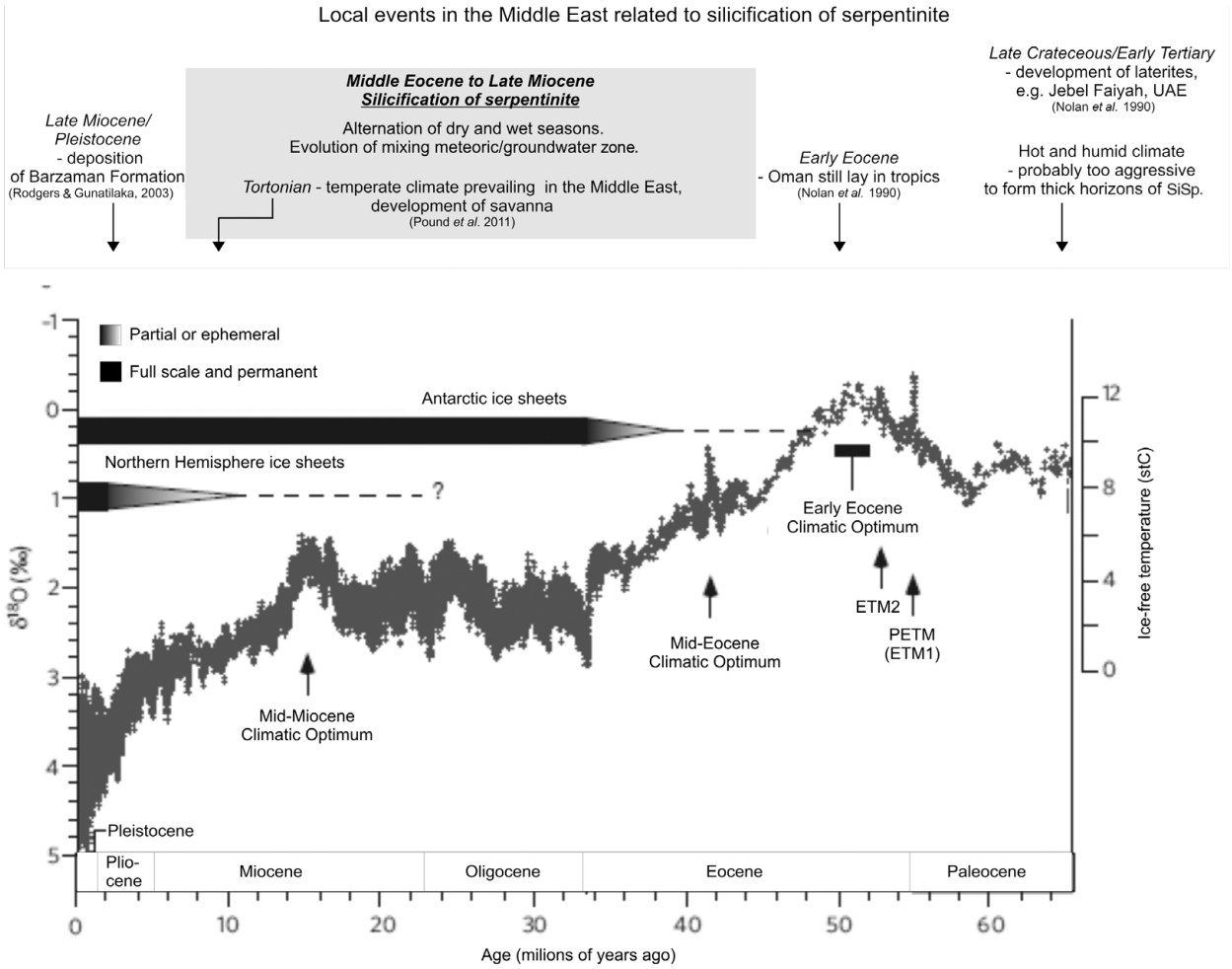

Figure 7. Diagram showing main global climatic events and local events related to silicification of serpentinite (modified after Zachos, Dickens & Zeebe, 2008). The climate curve (0–65 Ma) is a stacked deep-sea benthic foraminiferal oxygen-isotope curve based on records from Deep Sea Drilling Project and Ocean Drilling Program sites, updated with high-resolution records for the interval spanning the middle Eocene to the middle Miocene (Zachos, Dickens & Zeebe, 2008). The temperatures in the UAE would have been higher than the global average shown on the diagram. (PETM, ETM1 – Eocene Thermal Maximum 1; ETM2 – Eocene Thermal Maximum 2).

Formation). The silicification must have therefore taken place within a time span between the obduction of the ophiolite (Maastrichtian) and the deposition of the Barzaman Formation (late Miocene/Pliocene; Rodgers & Gunatilaka, 2003). In mid-Miocene time, the Neotethys Ocean finally closed (Styles *et al*. 2006).

Our study implies that the SiSp formed in a climate of alternating wet and dry seasons (temperate climate) and prior to deposition of the Barzaman Formation (late Miocene/Pliocene). The alternating wet and dry seasons provide conditions that could favour formation of a meteoric–groundwater mixing zone. The enhanced evaporation drives the hyperalkaline groundwater towards the bedrock surface where it then mixes with the meteoric water during the rainfall-dominated periods. The current climate in the Middle East is hot and dry with sparse and intermittent rainfall. The global climate in the Tertiary Period is known to have fluctuated from very warm in the Paleocene and Eocene (Eocene Climatic Optimum, 52–50 Ma) to cooler in the late Eocene and early Oligocene, and again warmer in end-Oligocene/Miocene times (Fig. 7). This warm phase peaked in the late middle Miocene climatic optimum (Zachos, Dickens & Zeebe, 2008). Subsequently, there was a gradual cooling down towards the beginning of the Quaternary Period.

On the Arabian Peninsula during late Campanian/early Maastrichtian to early Tertiary times, the climate is reported to have been hot and humid, and this is supported by the presence of thick lateritic profiles in Oman (Nolan *et al*. 1990) and in the UAE at Jebal Fayah. During early Eocene time, Oman still lay in the tropics (Nolan *et al*. 1990). This wet tropical climate of the Late Cretaceous and early Tertiary is considered to have generated highly acidic waters that could potentially be suitable for the formation of laterites but not for the formation of thick silcrete horizons, such as the SiSp.

The SiSp could have therefore formed during the time span (*c*. 40 Ma) from the middle Eocene to late Miocene. The climatic data for this period is scarce for the Arabian Peninsula; however, the presence of

https://doi.org/10.1017/S0016756812000325 Published online by Cambridge University Press

temperate savannah in the Middle East during the late Miocene Tortonian Age (Pound *et al*. 2011) confirms that the climate was moderate with alternating wet and dry seasons. These climatic conditions could have persisted for a much longer time than just the Tortonian. The global temperature graph by Zachos, Dickens & Zeebe (2008) implies gradual cooling starting in middle Eocene times. The global cooling could in turn mean a change in the Arabian Peninsula's climate from tropical to temperate. The alternations in a yearly cycle of wet and dry periods in a temperate climate could significantly affect the groundwater levels and induce the formation of a mixing zone with near-neutral pH suitable for the formation of silicified serpentinite.

8. Conclusions

(1) The silicified serpentinite in the UAE forms a continuous belt that is best exposed along the western piedmont of the Hajar Mountains. The thickness of the SiSp horizon varies from locality to locality, but usually does not exceed 5 m.

(2) The silicification preserved the original mesh texture characteristic of serpentinite. The well-preserved mesh texture probably resulted from a combination of iso-volumetric processes of slow rate dissolution of Mg-silicates and immediate local precipitation of silica. The rock is now composed of $>$ 95 % quartz and $<$2 % goethite + haematite, with trace amounts of clay minerals and residual chromites.

(3) The silicified horizon formed in a zone of mixing of meteoric and groundwaters, which mingled and produced mineralizing fluids of near-neutral pH. This environment favoured the precipitation of either opal (oversaturated fluids) or microquartz (less concentrated fluids), and proved to be stable, leading to complete silicification.

(4) The SiSp formed through incongruent dissolution of serpentine. The process involved initial preferential leaching of Mg and the formation of siliceous micro-seeds of either opal (subsequently transformed to microquartz) or microquartz. The siliceous micro-seeds have subsequently been overgrown by silica leached from weathered horizons elsewhere, perhaps from an overlying regolith.

(5) The SiSp represents a silcrete that is a part of palaeo-weathering surface residuum that probably developed in a temperate climate during middle Eocene to late Miocene times.

Acknowledgements. The authors wish to acknowledge J. Rushton, B. Rawlins, R. Ellison and A. Farrant, whose comments and suggestions greatly improved the manuscript. Thanks to D. Flight for her support, to D. Wagner for conducting the XRD analysis and to C. Gowing, S. Chenery, T. Barlow and M. Allen for conducting major and trace element analysis. We also thank J. Zachos for permission to publish the climate curve (0–65 Ma). The paper is published with the permission of the Executive Director of the British Geological Survey (Natural Environment Research Council).

References

ALSHARHAN, A. S. & NAIRN, A. E. M. 1990. A review of the Cretaceous formations in the Arabian Peninsula and Gulf: Part III. Upper Cretaceous (Aruma Group) stratigraphy and paleogeography. *Journal of Petroleum Geology* **13**, 247–66.

BARNES, I. & O'NEIL, J. R. 1978. Present day serpentinisation in New Caledonia, Oman and Yugoslavia. *Geochimica et Cosmochimica Acta* **42**, 144–5.

BARNES, I., O'NEIL, J. R., RAPP, J. B. & WHITE, D. E. 1973. Silica-carbonate alteration of serpentinite: wall rock alteration in mercury deposits of the California Coast Ranges. *Economic Geology* **68**, 388–98.

BARROS DE OLIVEIRA, S. M., TRESCASES, J. J. & MELFI, A. J. 1992. Lateritic deposits of Brazil. *Mineralium Deposita* **27**, 137–46.

BASSETT, H. 1954. Silicification of rocks by surface waters. *American Journal of Science* **252**, 733–5.

FOLK, R. L. & MCBRIDE, E. F. 1978. Radiolarites and their relation to subjacent "oceanic crust" in Liguria, Italy. *Journal of Sedimentary Petrology* **48**, 1069–102.

FLÖRKE, O. W., GRAETSCH, H., MARTIN, B., RÖLLER, K. & WIRTH, R. 1991. Nomenclature of micro- and non-crystalline silica minerals, based on structure and microstructure. *Neues Jahrbuch Mineralogische Abhandlung* **163**, 19–42.

GLENNIE, K. W., BOEUF, M. G. A., HUGHES CLARKE, M. W., MOODY-STUART, M., PILAAR, W. F. H. & REINHARDT, B. M. 1974. *Geology of the Oman Mountains*. The Royal Dutch Geological and Mining Society.

ILER, R. K. 1979. *The Chemistry of Silica*. New York: Wiley, 896 pp.

LEBLANC, M. & BILLAUD, P. 1982. Cobalt arsenide ore bodies related to an upper Proterozoic ophiolite: Bou Azzer (Morocco). *Economic Geology* **77**, 162–75.

LIU, Y., OLSEN, A. A. & RIMSTIDT, J. D. 2006. Mechanism for the dissolution of olivine series minerals in acidic solutions. *American Mineralogist* **91**, 455–8.

LUCE, R. W., BARTLETT, R. W. & PARKS, G. A. 1972. Dissolution kinetics of magnesium silicates. *Geochimica et Cosmochimica Acta* **36**, 35–50.

MOLLY, E. W. 1959. Platinum deposits of Ethiopia. *Economic Geology* **54**, 467–77.

NASIR, S., AL SAYIGH, A. R., AL HARTHY, A., AL-KHIRBASH, S., AL-JAAIDI, O., MUSLLAM, A., AL-MISHWAT, A. & AL-BU'SAIDI, S. 2007. Mineralogical and geochemical characterization of listwaenite from the Semail Ophiolite, Oman. *Chemie der Erde* **67**, 213–28.

NICKEL, E. H. & THORNBER, M. R. 1977. Chemical constrains on the weathering of serpentinites containing nickel-iron sulphides. *Journal of Geochemical Exploration* **8**, 235–45.

NOLAN, S. C., SKELTON, P. W., CLISSOLD, B. P. & SMEWING, J. D. 1990. Maastrichtian to early Tertiary stratigraphy and palaeogeography of the central and northern Oman Mountains. In *The Geology and Tectonics of the Oman Region* (eds A. H. F. Robertson, M. P. Searle & A. C. Ries), pp. 495–519. Geological Society of London, Special Publication no. 49.

OTTEMANN, J. & AUGUSTITHIS, S. S. 1967. Geochemistry and origin of "Platinum-Nuggets" in lateritic covers from ultrabasic rocks and birbirites of W. Ethiopia. *Mineralium Deposita* **1**, 260–77.

POKROVSKY, O. S. & SCHOTT, J. 2000. Forsterite surface composition in aqueous solutions: a combined potentiometric, electrokinetic, and spectroscopic approach. *Geochimica et Cosmochimica Acta* **64**, 3299–312.

POUND, M. J., HAYWOOD, A. M., SALZMANN, U., RIDING, J. B., LUNT, D. J. & HUNTER, S. 2011. A Tortonian (Late Miocene, 11.61–7.25 Ma) global vegetation reconstruction. *Palaeogeography, Palaeoclimatology, Palaeoecology* **300**, 29–45.

RICE, S. J & CLEVELAND, G. B. 1955. Lateritic silification of serpentinite in the Sierra Nevada. *Geological Society America Bulletin* **66**, 1660.

RODGERS, D. W. & GUNATILAKA, A. 2003. Bajada formation by monsoonal erosion of a subaerial forebulge, Sultanate of Oman. *Sedimentary Geology* **154**, 127–46.

ROSSO, J. J. & RIMSTIDT, J. D. 2000. A high resolution study of forsterite dissolution rates. *Geochimica et Cosmochimica Acta* **64**, 797–811.

SIEVER, R. & WOODFORD, N. 1979. Dissolution kinetics and weathering of mafic minerals. *Geochimica et Cosmochimica Acta* **43**, 717–24.

SHAETZL, R. J. & ANDERSON, S. 2005. *Soils: Genesis and Geomorphology*. Cambridge: Cambridge University Press.

SOM, S. K. & JOSHI, R. 2002. Chemical weathering of serpentinite and Ni enrichment in Fe oxide at Sukinda Area, Jajpur District, Orissa, India. *Economic Geology* **97**, 165–72.

SNYDER, R. L. & BISH, D. L. 1989. Quantitative analysis. In *Modern Powder Diffraction* (eds D. L. Bish & J. E. Post), pp. 101–44. *Reviews in Mineralogy*, vol. **20**. Washington DC: Mineralogical Society of America.

STEIN, C. L. & KIRKPATRICK, R. J. 1976. Experimental porcelanite recrystalisation kinetics: a nucleation and growth model. *Journal of Sedimentary Petrology* **46**, 430–5.

STANGER, G. 1985. Silicified serpentinite in the Semail nappe of Oman. *Lithos* **18**, 13–22.

STYLES, M. T., ELLISON, R. A., ARKLEY, S. L. B., CROWLEY, Q. G., FARRANT, A., GOODENOUGH, K. M., MCKERVEY, J. A., PHARAOH, T. C., PHILLIPS, E. R., SCHOFIELD, D. & THOMAS, R. J. 2006. *The Geology and Geophysics of the United Arab Emirates*: *Volume 2*, *Geology*. Abu Dhabi, United Arab Emirates: UAE Ministry of Energy, 351 pp.

THIRY, M. & MILLOT, G. 1986. Mineralogical forms of silica and their sequence of formation in silcretes. *Journal of Sedimentary Petrology* **57**, 343–52.

THIRY, M. & SIMON-COINCON, S. 1996. Tertiary paleoweatherings and silcretes in the southern Paris Basin. *Catena* **26**, 1–26.

THIRY, M. & SIMON-COINCON, S. 1999. Diversity of continental silicification features: examples from the Cenozoic deposits in the Paris Basin and neighbouring basement. In *Paleoweathering, Paleosurfaces and Related Continental Deposits*, pp. 87–127. Special Publication of the International Association of Sedimentologists no. 27.

TRESCASES, J. J. 1973. Weathering and geochemical behaviour of the elements of ultramafic rocks in New Caledonia. Bureau of Mineral Resources, Geology and Geophysics, Canberra, Extract from Bulletin 141, pp. 149–161.

VENTURELLI, G., CONTINI, S. & BONAZZI, A. 1997. Weathering of ultramafic rocks and element mobility at Mt. Prinzera, Northern Apennines, Italy. *Mineralogical Magazine* **61**, 765–78.

WILLIAMS, L. A., PARKS, G. A. & CRERAR, D. A. 1985. Silica diagenesis; I, Solubility controls. *Journal of Sedimentary Petrology* **55**, 301–11.

ZACHOS, J., DICKENS, G. M. & ZEEBE, R. E. 2008. An early Cenozoic perspective on greenhouse warming and carbon-cycle dynamics. *Nature* **451**, 279–83.